Dependence of the Omori-Utsu aftershock law on mainshock magnitude

Sebastian Hainzl[1] and David Marsan[2]

[1] Deutsches GeoForschungsZentrum, Potsdam, Germany
[2] LGIT, University of Savoie, Le Bourget du Lac, France

SAFER
Seismic eArly warning For EuRope

INTRODUCTION

We examine the dependence on M of the p and χ parameters appearing in Omori-Utsu formula

$$R(t,M) = \chi \cdot (t+c)^{-p}$$

relating the rate of aftershocks R at time t after a mainshock of magnitude M. Observations point out to a significant increase of p with M, along with a scaling relationship of the form $\chi \sim 10^{\alpha M}$. We here show that these observations can be explained within the framework of the rate-and-state friction model, when accounting for realistic levels of coseismic stress heterogeneity on the main fault. We constrain the model parameters in order to recover the trends observed in previous and new analyses of aftershock sequences. Finally, the influence of afterslip on parameters p and χ is studied, to highlight the fact that it can significantly perturb the $p(M)$ and $\chi(M)$ relations obtained with the initial afterslip-free model.

I. Slip & Stress Heterogeneities

Slip on the rupture plane is found to be scale-invariant, $\mathbf{u(k)} \propto \mathbf{k^{-1-H}} \cdot \lambda(\mathbf{k})$ (Mai & Beroza 2002), where k the wave number; $H = 3 - D$ is the Hurst exponent; and λ Gaussian white noise. This leads to stress field variation on the length scale of the nucleation sites l with a standard deviation (Marsan 2006):

$$\sigma \sim \sqrt{\left(\frac{\mathbf{L}}{\mathbf{l}}\right)^{\mathbf{2-2H}} - \mathbf{1}} = \sqrt{\mathbf{10^{0.9(M-M_l)(1-H)}} - \mathbf{1}} \quad (1)$$

with $M(L) = c + \log(L)/0.45$ (Wells & Coppersmith 1994)

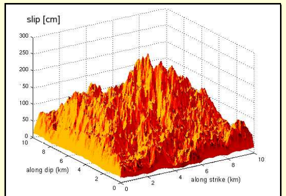

Fig.1: Example for a slip distribution at the 40m scale (H=0.7) for a 10kmx10km strike-slip fault.

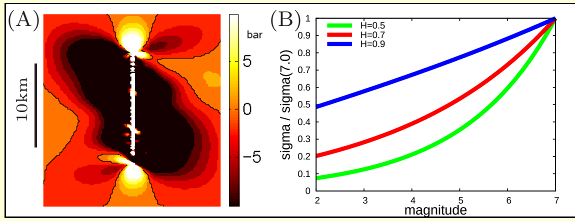

Fig.2: (A) Coulomb stress change at 5km depth for the example in Fig.1 with a friction coefficient of 0.4. (B) The dependence of the expected rupture induced stress drop variability on the earthquake magnitude.

II. Earthquake Nucleation

The frictional strength of faults depends on the rate and state variables according to

$$\mu(t) = \mu_0 + A\ln\left(\frac{v(t)}{v_0}\right) + B\ln\left(\frac{v_0\Theta(t)}{L_0}\right) \quad \& \quad \frac{\partial\Theta}{\partial t} = 1 - \frac{v(t)\Theta(t)}{L_0}$$

where A, B, v_0 and L_0 are constants, and v is slip velocity.
For a population of faults, a sudden stress jump τ leads to a time-dependent earthquake activity according to (Dieterich 1994)

$$\mathbf{R(t,\tau) = r/[1 + (e^{-\tau} - 1)e^{-t}]} \quad (2)$$

where r is the background rate. Stresses are given in units of $A\sigma$ and time in units of $A\sigma/\dot{\tau}$ (tectonic loading rate $\dot{\tau}$; effective normal stress σ). Because the induced stress changes have a (mainshock) magnitude-dependent variability (see Sec.I), the total rate becomes

$$\mathbf{R(t,M)} = \frac{\mathbf{1}}{\sqrt{\mathbf{2\pi}}\sigma_\mathbf{M}} \int_{-\infty}^{\infty} \mathbf{R(t,\tau)} e^{-\frac{(\tau-\bar{\tau})^2}{2\sigma_M^2}} \, \mathbf{d\tau} \quad (3)$$

III. Magnitude-Dependence of the Aftershock Decay

In the following, we assume that the average stress drop is $\bar{\tau} = 10A\sigma$ and define the stress variability σ_7 (at length scale of nucleation) induced by a M7 event as an input variable. The numerical solution of Eq.(3) yields:

The productivity as well as the shape of the aftershock decay is strongly magnitude-dependent.

This is shown in **Fig.3** for the case of H=0.7 and $\sigma_7 = 2.3\,\bar{\tau}$.

(A) The p-value increases with mainshock magnitude which is in good agreement with the observed p-value dependence in California [Ouillon and Sornette, 2005] and our own analysis of the global ISC earthquake catalog. This is shown in **Fig.4**, where brown and red points mark the California data for two different declustering methods and green crosses refer to the global data set. The lines correspond to a stress field heterogeneity $\sigma_7 = 6.5\,\bar{\tau}$ (H=0.5); $\sigma_7 = 2.3\,\bar{\tau}$ (H=0.7), and $\sigma_7 = \bar{\tau}$ (H=0.9).

(B) The aftershock density increases with mainshock magnitude and the total productivity increases approximately with $10^{1.05M}$ which is similar to a previous result for California, α=1.05±0.05 [Helmstetter et al., 2005]. However, please note that different mainshock-aftershock definitions can lead to quite different α-estimations. **Fig.5** shows the productivity χ as a function of mainshock magnitude in comparison with the values observed in the global earthquake catalog.

Fig.3

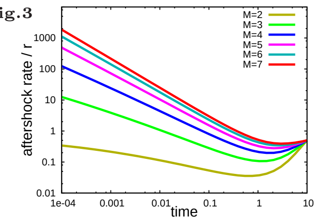

Fig.4

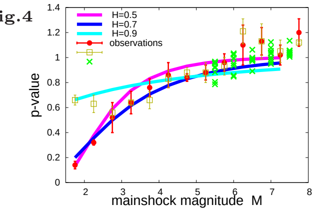

Fig.5

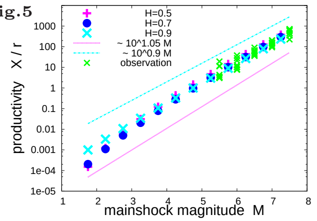

IV. Impact of afterslip

There is growing evidence that large mainshocks are followed by significant amount of afterslip decaying with $1/t$. Therefore we explore the impact of postseismic stress changes according to

$$\tau(t) = \tau_0 + \tau_1 \cdot \ln(1 + t/t^*)$$

where t^* is set to $10^{-7}\,t_a$. For the same parameters as before (H=0.7; $\bar{\tau}$=10; σ_7=23), **Fig.6** shows the p-value increase for different ratios $\tau_1 \ln(1 + t_a/t^*)/\tau_0$: p-values larger than 1 are found in the case of very strong unloading when the afterslip induced stress reduction is of the order of the coseismic mean stress drop.

Fig.6

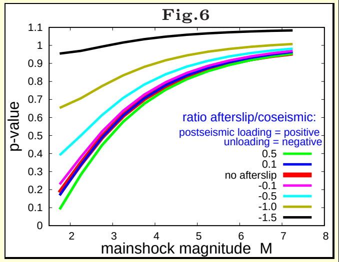

SUMMARY

The rate-and-state dependent friction model has already been shown to explain several aspects of triggered seismicity such as aftershock activity according to the Omori-Utsu law. In the same framework, rupture induced stress heterogeneities have been identified as a possible explanation for aftershocks occurring in stress shadows. Here, we show that these induced heterogeneities are expected to be size-dependent and thus the aftershock decay should be dependent on the mainshock magnitude: The p-value and the aftershock density increases with M. We find that the model predictions are in good agreement with observations. Furthermore, we show that log(t)-unloading in agreement with frequently observed afterslip can explain $p > 1$, however, the general trend of the p-value and aftershock density increase with mainshock-magnitude remains unchanged by afterslip.

Dieterich, J. H. (1994), *J. Geophys. Res.*, *99*, 2601–2618.
Hainzl, S. & Marsan, D. (2008), *J. Geophys. Res.*, *113*, B10309, doi:10.1029/2007JB005492.
Helmstetter, A., Kagan, Y.Y. & Jackson, D.D. (2005), *J. Geophys. Res.*, *110*, B05S08, doi:1029/2004JB003286.
Mai, P. M. & Beroza, G. C. (2002), *J. Geophys. Res.*, *107*, 2308, doi:10.1029/2001JB000588.
Marsan, D. (2006), *J. Geophys. Res.*, *111*, B06305, doi:10.1029/2005JB004060.
Ouillon, G. & Sornette, D. (2005), *J. Geophys. Res.*, *110*, B04306, doi:10.1029/2004JB003311.